The baroclinic instability of a mid-ocean circulation

By ELLIOTT E. SCHULMAN, *Pierce Hall, Harvard University, Cambridge, Massachusetts*

(Manuscript received September 15, 1966)

ABSTRACT

The instability of a flow modelling a linear oceanic thermocline is investigated with a view towards understanding the intermediate-scale fluctuations observed by Crease (1962) and others. Robinson's (1962) analysis of the stability of a thermal ocean circulation is extended to include amplifying quasi-geostrophic perturbations. North–south wavelengths of several hundred kilometers are predicted and agree with previous measurements.

For the special case of perturbations independent of longitude, a uniformly valid solution is obtained for oceans of large latitudinal extent. Growth rates are of the order of one year, and the north–south wavelength is a function of latitude.

Although the basic state chosen is different from its atmospheric counterpart examined by Eady (1949) and Green (1960), both are baroclinically unstable and have perturbations with similar properties. At maximum instability, both have perturbations which are constant in the direction parallel to the basic lateral density gradient, and this result is true both on an f-plane and β-plane.

I. Introduction

It has been established by means of neutrally buoyant floats (Swallow, 1955) and improved velocity meters, that the deep mid-ocean circulation is not slow and steady as had been previously thought, but exhibits large fluctuations in space and time. For example, Crease (1962) found currents of the order of 10 cm/sec in deep water (2000 m and 4000 m) off Bermuda which had significant changes in direction over a period of several months, and which apparently have a horizontal length scale of at least 40 nautical miles. Day & Webster (1965), taking detailed measurements at one location in the Sargasso Sea, found in addition to inertia-gravity oscillations, a large time scale fluctuation in the circulation. The latter had a period greater than three months (the time over which observations were taken) and had average speeds of about 20 cm/sec at 50 and 100 m.

There is no external driving force which corresponds to these fluctuations whose magnitude is much greater than any steady component. One explanation is that this phenomenon is the manifestation of an instability in the mean, mid-ocean circulation—a possibility that will be explored in this paper.

The open ocean circulation is characterized by the thermocline field which is too complicated in its full description (Robinson & Stommel, 1959; Welander, 1959) to permit a stability analysis. We shall instead consider a simplified model of the ocean which is more amenable to analytical methods and yet which contains some essential features of the thermal circulation.

For geostrophic motion on a β-plane in which the hydrostatic and Boussinesq approximations are valid, the thermal wind relation

$$W'_{zz} = -\frac{\beta g}{f'^2}\frac{\partial \varrho'}{\partial x} \tag{1.1}$$

can be derived where W' = vertical velocity, g = gravitational acceleration, f' = Coriolis parameter, $\beta = df'/dy$, ϱ' = density and x, y, z are the longitudinal, latitudinal, and vertical coordinates respectively.

Robinson & Stommel (1959) showed that a vertical velocity is necessary to support the oceanic thermocline. From (1.1), a longitudinal density gradient is required. In other words, the surface latitudinal density gradient produced by insolation is twisted into a longitudinal

This research was supported by the National Science Foundation, in part by NSF grant G-24903 (Atmospheric Sciences Section) and in part by NSF grant GP 3533 (Oceanic Dynamics), both to Harvard University.

gradient in the thermocline. In the subsequent analysis, we shall assume that the latter, combined with a vertical density stratification, contains the relevant properties of the thermocline and is the driving force of the basic state whose instability will be investigated.

This basic state was employed by Robinson (1962) in his discussion of neutrally stable geostrophic perturbations. His analysis will be continued and extended to the more physically interesting case of quasigeostrophic perturbations which are growing.

In this model, a vertical density gradient extends from the top to bottom, at which boundaries the vertical velocity is prescribed to vanish. In the real oceans however, most of the density difference occurs in the thermocline. Making this the vertical scale gives a more realistic density distribution, but now there is no justification for setting the vertical velocity to zero at this depth. As a compromise between these two physical requirements, a value (3 km) intermediate to the thermocline depth (1 km) and oceanic depth (5 km) is chosen in the calculations. In Section IX, the effect of varying choices of vertical scale will be examined more closely.

In the following analysis, we will deal with ocean circulations in which the Boussinesq and β-plane approximations are valid. Boundary conditions on the sides of the ocean basins which require boundary layers and vanishing of normal velocities will be ignored: we will be concerned solely with the stability properties of the interior, mid-ocean flow.

II. The basic state

In the Atlantic (Defant, 1961, Chapter V) and Pacific (Reid, 1965) there is observed a positive density difference from the western to eastern boundaries of the oceans equal to about 2×10^{-3} g/cm^3 at the surface and decreasing to zero at the bottom. For simplicity, we shall in this model consider only a constant longitudinal density gradient at all levels. Instead of working with density ϱ' as a dependent variable, we shall use apparent temperature ϑ'. Thus our basic state will have a negative apparent temperature gradient to the east since $\Delta\varrho' = -\alpha g\,\Delta\vartheta'$.

The boundary conditions prescribed for the basic state are:

$$\vartheta' = -(\Delta T)_H \frac{x}{L} \quad \text{at} \quad z=0, \tag{2.1}$$

$$\vartheta' = -(\Delta T)_H \frac{x}{L} + (\Delta T)_v \quad \text{at} \quad z=H, \tag{2.2}$$

$$W'=0 \quad \text{at} \quad z=0 \quad \text{and} \quad z=H, \tag{2.3}$$

where L and H are the characteristic longitudinal and vertical scales, and $(\Delta T)_H$ and $(\Delta T)_v$ are the corresponding apparent temperature differences. Note that as defined they are both positive quantities. The existence of continents bounding the ocean on either side is implicit in the assumption of a longitudinal temperature gradient and the use of the length scale L. No boundary conditions will be applied on vertical latitudinal surfaces and the characteristic north–south length M is chosen to be equal to the planetary scale, i.e., $M=f_0/\beta$.

To non-dimensionalize, choose

$$x=L\xi^*, \quad y=M\eta^*, \quad z=H\zeta \tag{2.4}$$

and

$$\left.\begin{aligned} &U'=V_0\frac{L}{M}U, \quad V'=V_0V, \quad W'=V_0\frac{H}{M}W,\\ &\vartheta'=(\Delta T)_H\vartheta, \quad f'=f_0f, \end{aligned}\right\} \tag{2.5}$$

in which V_0, the characteristic velocity, is equal to $\alpha g(\Delta T)_H H/f_0 L$, where α = thermal expansion coefficient and f_0 is the Coriolis parameter in the center of the ocean basin ($y=0$). The non-dimensional equations governing the basic state are then

$$-fV+\gamma^2R_0\mathfrak{L}(U)+P_{\xi^*}=0, \tag{2.6}$$

$$fU+R_0\mathfrak{L}(V)+P_{\eta^*}=0, \tag{2.7}$$

$$-\vartheta+P_\zeta=0, \tag{2.8}$$

$$U_{\xi^*}+V_{\eta^*}+W_\zeta=0, \tag{2.9}$$

$$-\vartheta_{\zeta\zeta}+\Lambda\mathfrak{L}(\vartheta)=0, \tag{2.10}$$

where $\mathfrak{L}=U(\partial/\partial\xi^*)+V(\partial/\partial\eta^*)+W(\partial/\partial\zeta)$. The boundary conditions are

$$\vartheta=-\xi^* \text{ at } \zeta=0, \tag{2.11}$$

$$\vartheta=-\xi^*+\theta \text{ at } \zeta=1, \tag{2.12}$$

$$W=0 \text{ at } \zeta=0 \text{ and } \zeta=1. \tag{2.13}$$

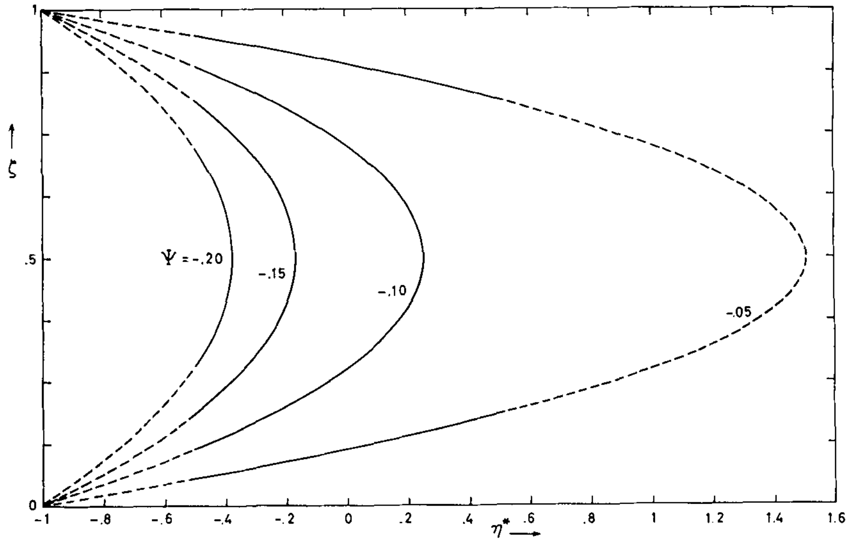

Fig. 1. Streamlines of the basic state. North is in the direction of increasing η^*, and $\eta^* = -1$ corresponds to the equator. The full lines indicate the approximate region of validity for solutions on the β-plane.

The above non-dimensional parameters are

$R_0 = \dfrac{V_0}{f_0 L}$ (the Rossby number of the basic flow),

$\gamma = \dfrac{L}{M}$,

$\Lambda = \dfrac{V_0 H^2}{\varkappa M}$ (the Péclet number of the basic flow based on the horizontal temperature difference)

and $\theta = \dfrac{(\Delta T)_V}{(\Delta T)_H}$.

For typical ocean values ($L = 6 \times 10^8$ cm, $M = 3 \times 10^8$ cm, $f_0 = 10^{-4}$ sec^{-1}, $V_0 = 1$ cm/sec, $H = 3 \times 10^5$ cm, $\varkappa = 50$ cm^2/sec, $\alpha(\Delta T)_H = 2 \times 10^{-4}$, $\alpha(\Delta T)_V = 2 \times 10^{-3}$), R_0 is of the order of 10^{-5} and the other parameters are all between 0(1) and 0(10).

Neglect the non-linear momentum advections multiplied by the small parameter R_0 and assume the velocity field is independent of ξ^*. Then, if the longitudinal density gradient is constant, the apparent temperature is of the form

$$\vartheta = -\xi^* + \theta S(\eta, \zeta) \tag{2.14}$$

and the meridional and vertical velocities are given exactly by

$$V = -\frac{1}{f}(\zeta - \tfrac{1}{2}), \tag{2.15}$$

$$W = -\frac{1}{f^2}\left(\frac{\zeta^2}{2} - \frac{\zeta}{2}\right). \tag{2.16}$$

Introduce the streamfunction $\psi' = V_0 H \psi$ such that $V = -\psi_\zeta$ and $W = \psi_{\eta^*}$, then

$$\psi = \frac{1}{f}\left(\frac{\zeta^2}{2} - \frac{\zeta}{2}\right), \tag{2.17}$$

which is exhibited in Fig. 1. The vertical velocity is always upwards; the meridional velocity is southwards in the upper (higher) half of the ocean and northwards in the lower half. Note that the β-plane approximation is valid only for ocean regions at a distance less than f_0/β from the mid-latitude. The line $\eta^* = -1$ is the equatorial singularity of geostrophic flow.

If we assume that Λ is small enough that an expansion in it is valid, we find that

$$\vartheta = -\xi^* + \theta\zeta - \frac{\Lambda\theta}{12 f^2}\left(\frac{\zeta^4}{2} - \zeta^3 + \frac{\zeta^2}{2}\right) + \theta[G_2(f, \zeta)\Lambda^2 + \cdots], \tag{2.18}$$

$$U = -\frac{\Lambda\theta}{12 f^4}\left(\frac{\zeta^5}{5} - \frac{\zeta^4}{2} + \frac{\zeta^2}{2} - \frac{1}{10}\right) + \theta[H_2(f, \zeta)\Lambda^2 + \cdots], \tag{2.19}$$

in which the additional assumption of zero zonal transport has been made, i.e. $\int_0^1 U d\zeta = 0$.

The field represented by (2.15), (2.16) and the expansions (2.18) and (2.19) is the basic state whose stability will now be investigated.

III. Perturbation equations

The full linearized dimensional equations for the perturbation are

$$u_t' - f'v' + U'u_x' + V'u_y' + W'u_z' + U_y'v + U_z'w' + p_x' = 0, \quad (3.1)$$

$$v_t' + f'u' + U'v_x' + V'v_y' + W'v_z' + V_y'v + V_z'w' + p_y' = 0, \quad (3.2)$$

$$-\alpha g T' + p_z' = 0, \quad (3.3)$$

$$u_x' + v_y' + w_z' = 0, \quad (3.4)$$

$$T_t' - KT_{zz} + U'T_x' + V'T_y' + W'T_z' + \vartheta_x' u' + \vartheta_y' v' + \vartheta_z' w' = 0. \quad (3.5)$$

In the notation used in this paper, primed quantities refer to dimensional field variables, unprimed quantities to nondimensional variables. Upper case letters and ϑ refer to the basic state, lower case and T to the perturbations.

The length scale of the perturbations will in general be of a different order of magnitude from that of the basic state. Anticipating this result, it is found to be convenient to scale the perturbations with respect to the order of their wavelengths:

$$x = \frac{1}{\lambda_0}\xi, \quad (3.6)$$

$$y = \frac{1}{\mu_0}\eta, \quad (3.7)$$

$$z = H\zeta, \quad (3.8)$$

and

$$t = \frac{1}{\mu_0 V_0}\tau, \quad (3.9)$$

where $2\pi/\lambda_0$ and $2\pi/\mu_0$ are the east–west and north–south wavelengths respectively, evaluated at the mid-latitude of the ocean, $y = 0$. The actual wavelengths may in fact be functions of the latitude.

Similarly, to preserve three-dimensionality in the continuity equation, the perturbations are non-dimensionalized

$$u' = V_0 \frac{\mu_0}{\lambda_0} u, \quad (3.10)$$

$$v' = V_0 v, \quad (3.11)$$

$$w' = V_0 H \mu_0 w, \quad (3.12)$$

$$T' = (\Delta T)_H T. \quad (3.13)$$

In this formulation there are two non-dimensional coordinates in the north–south direction:

$$\eta^* = y/M, \quad (3.14)$$

which varies by 0(1) over the entire ocean basin and η, given by (3.7), scaled with respect to the perturbation wavelength. Then

$$\eta^* = \varepsilon\eta, \quad (3.15)$$

where

$$\varepsilon = \frac{1}{\mu_0 M} \quad (3.16)$$

is the ratio of the perturbation-wavelength to the planetary scale. Consequently,

$$f = 1 + \eta^* \quad (3.17)$$

and

$$\frac{\partial f}{\partial \eta} = \varepsilon. \quad (3.18)$$

If many north–south waves are contained in the ocean-basin, ε is much less than 1. Equations (3.1) to (3.5) then become in non-dimensional form:

$$-fv + p_\xi + \frac{R_0}{\varepsilon}\frac{\gamma^2}{r}[u_\tau + rUu_\xi + Vu_\eta + \varepsilon W u_\zeta + \varepsilon r v U_{\eta^*} + rU_\zeta w] = 0, \quad (3.19)$$

$$fu + p_\eta + \frac{R_0}{\varepsilon} r[v_\tau + rUv_\xi + Vv_\eta + \varepsilon W v_\zeta + \varepsilon V_{\eta^*} v + V_\zeta w] = 0, \quad (3.20)$$

$$-T + \frac{\varepsilon}{r} p_\zeta = 0, \quad (3.21)$$

$$u_\xi + v_\eta + w_\zeta = 0, \quad (3.22)$$

$$-\frac{\varepsilon}{\Lambda}T_{\zeta\zeta}+T_\tau+rUT_\xi+VT_\eta+\varepsilon WT_\zeta$$
$$+\frac{\varepsilon}{r}\vartheta_{\xi*}u+\varepsilon\vartheta_{\eta*}v+\vartheta_\zeta w=0, \quad (3.23)$$

where $r=\lambda_0 L/\mu_0 M$ is the ratio of the number of east-west waves to north-south waves enclosed in the ocean.

The appropriate boundary conditions are simply

$$w=0 \text{ at } \zeta=0, \text{ and } \zeta=1 \quad (3.24)$$

and
$$T=0 \text{ at } \zeta=0, \text{ and } \zeta=1. \quad (3.25)$$

IV. Geostrophic perturbations

If we assume that ε and r do not take on extreme values (either very small or very large), then for small R_0, the local accelerations and momentum advections can be ignored and the perturbation flow is geostrophic. Equations (3.19) to (3.23) can then be combined into a single fourth order differential equation in w equivalent in form to equation (29) in Robinson (1962) but with parameters modified by the different choice of non-dimensional variables.

Since $T_\xi=(f^2/r)w_{\zeta\zeta}$, the appropriate boundary conditions (3.24) and (3.25) become

$$w=w_{\zeta\zeta}=0 \text{ at } \zeta=0 \text{ and } \zeta=1. \quad (4.1)$$

If we set $f=1$ in the final equation but also retain all terms that arose from previous differentiations, the coefficients are functions only of the independent variable ζ, and a wave form for the perturbation, $w=\omega(\zeta)e^{i(\sigma\tau+\eta+\xi)}$ is permissible. Since the basic state is given by an infinite series, it is instructive to compare the growth rates and frequencies for various places of truncation of the series. The Galerkin procedure described by Robinson (1962) was used to solve the boundary value problem but with five Fourier modes in the vertical to achieve better accuracy. Briefly summarizing the results, we find:

1. For relatively small values of $\Lambda(\Lambda\lesssim5)$ the growth rates as functions of the parameters for the series (2.18) and (2.19) are quantitatively close to that of the non-series basicstate

$$\vartheta=-\xi^*+\theta\zeta, \quad (4.2)$$
$$U=0. \quad (4.3)$$

For the value $\Lambda=10$ however, no meaningful results were obtained, the series being divergent or too slowly convergent to be of use. Results are valid then only for $\Lambda\lesssim5$, and in particular, if we wish to use the simplified mean state (4.2) and (4.3) which describes a thermocline dominated by diffusion, we must confine the analysis to well within this range. Alternatively, if this maximum permissible Λ is specified, V_0 is about 1 cm/sec for $H=3\times10^5$ cm and $\varkappa=50$ cm^2/sec.

2. All waves are stable for values of Λ/ε below some critical number which is approximately 125 for typical ocean values. The ratio Λ/ε is the Péclet number based on the perturbation length scale.

3. For each ε, there exists a value of r for which the growth rates are a maximum.

4. As ε decreases to zero, the growth rates increase without limit (and are in fact, inversely proportional to ε).

V. Small wave-length expansion

Of especial interest is the last conclusion since we expect that waves with maximum growth rates will predominate in the circulation. However, the above stability analysis is not correct as ε decreases to $0(R_0^{1/2})$ because the momentum advections and local accelerations can then no longer be consistently neglected.

Letting $S=(R_0/\varepsilon^2)\gamma^2$ and restricting the basic state to small values of $\Lambda(\lesssim5)$ such that (4.2) and (4.3) are valid approximations, the equations of motion (3.19) to (3.23) become

$$-(1+\eta^*)v+p_\xi+\frac{S}{r}\varepsilon(u_\tau+Vu_\eta+\varepsilon Wu_\zeta)=0, \quad (5.1)$$

$$(1+\eta^*)u+p_\eta+\frac{Sr}{\gamma^2}\varepsilon(v_\tau+Vv_\eta+\varepsilon Wv_\zeta$$
$$+\varepsilon V_{\eta*}v+V_\zeta w)=0, \quad (5.2)$$

$$-T+\frac{\varepsilon}{r}p_\zeta=0, \quad (5.3)$$

$$u_\xi+v_\eta+w_\zeta=0, \quad (5.4)$$

$$-\frac{\varepsilon}{\Lambda}T_{\zeta\zeta}+T_\tau+VT_\eta+\varepsilon WT_\zeta-\frac{\varepsilon}{r}u+\theta w=0. \quad (5.5)$$

From its definition, $S=[\alpha g(\Delta T)_H/f_0^2]\mu_0^2$ and is $0(1)$ when

$$\frac{1}{\mu_0} = 0\left(\frac{\alpha g(\Delta T)_H}{f_0^2}\right)^{\frac{1}{2}}, \tag{5.6}$$

the deformation radius based on the lateral temperature difference. The characteristic number B discussed by Phillips (1963) is by definition equal to $R_0'^2 Ri'$ where

$R_0' = \frac{V_0}{f_0}\mu_0$ (the perturbation Rossby number),

$Ri' = \frac{\alpha g(\Delta T)_H H}{V_0^2}$ (the perturbation Richardson number)

and hence

$$B = \theta S. \tag{5.7}$$

Equations (5.1) to (5.5) are the relevant form of the perturbation equations. This set of five partial differential equations in the independent variables ξ, η, ζ and τ have coefficients which are functions only of ζ and $(1+\eta^*)$, since

$$V = -\frac{1}{(1+\eta^*)}(\zeta - \tfrac{1}{2}), \tag{5.8}$$

$$W = -\frac{1}{(1+\eta^*)^2}\left(\frac{\zeta^2}{2} - \frac{\zeta}{2}\right). \tag{5.9}$$

Ideally, we would like to obtain the solution to these equations with the full η^* dependence, specifying, in addition to the boundary conditions that w and T vanish at $\zeta = 0$ and $\zeta = 1$, some condition on the η-dependence, e.g. boundary conditions on two vertical latitudinal surfaces, or some periodicity condition in the η direction. However, the stability analysis of such a meridional-vertical circulation with both horizontal and vertical shear, is, except for special cases (see Section VIII) prohibitively difficult to solve by ordinary techniques.

In this problem, the north–south wavelength is much smaller than the radius of the earth, and even over several waves, the Coriolis parameter varies only slightly. If the ocean under consideration is of small latitudinal extent such that η^* is everywhere much less than 1, i.e. η is always 0(1), it is permissible to set f equal to a constant in the final stability equation—provided we have not neglected derivatives of f with respect to other $0(\varepsilon)$ quantities. Then a power expansion in the small parameter ε is valid, and the coefficients in the eigenfunction equation will now be functions of ζ only. In this "local" solution, stability properties of the perturbation will depend on β and the local value of f'.

For oceans of large latitudinal extent, the Coriolis parameter changes significantly from south to north, and a "local" solution implies that the growth rate is a function of latitude. This is an unsatisfactory result since the differential equations do not contain τ in the coefficients and we are seeking *one* value of the growth rate and frequency which characterizes the *entire* flow.

We shall here make the local hypothesis in the expectation that the slow latitudinal variations of the Coriolis parameter and basic state are of secondary importance to the vertical profile. Then, since $\eta^* = \varepsilon\eta < 1$, max $\{\eta^*\} < 1$, we may expand all field quantities in an ε expansion. This is equivalent to a quasigeostrophic approximation since the perturbation Rossby number, R_0' is equal to $(V_0/f_0)\mu_0 = (S/\gamma)\varepsilon$, or $0(Ro') = 0(\varepsilon)$ when S and γ are order 1. Let

$$u = u_0 + \varepsilon u_1 + \dots, \quad v = v_0 + \varepsilon v_1 + \dots, \quad \text{etc.} \tag{5.10}$$

Then to zeroth order, (5.1) to (5.5) become

$$-v_0 + p_{0\xi} = 0, \tag{5.11}$$

$$u_0 + p_{0\eta} = 0, \tag{5.12}$$

$$u_{0\xi} + v_{0\eta} = 0, \tag{5.13}$$

$$T_0 = 0, \tag{5.14}$$

$$w_0 = 0. \tag{5.15}$$

The horizontal velocities are geostrophic and non-divergent to lowest order and the stability problem is undetermined until we go to first order in ε:

$$-v_1 - \eta v_0 + p_{1\xi} + \frac{S}{r}(u_{0\tau} + Vu_{0\eta}) = 0, \tag{5.16}$$

$$u_1 + \eta u_0 + p_{1\eta} + \frac{Sr}{\gamma^2}(v_{0\tau} + Vv_{0\eta}) = 0, \tag{5.17}$$

$$-T_1 + \frac{1}{r}p_{0\zeta} = 0, \tag{5.18}$$

$$u_{1\xi} + v_{1\eta} + w_{1\zeta} = 0, \tag{5.19}$$

$$T_{1\tau} + VT_{1\eta} - \frac{1}{r}u_0 + \theta w_1 = 0. \tag{5.20}$$

Eliminate pressure by cross-differentiating (5.16) and (5.17) to obtain the vertical vorticity equation

$$-w_{1\zeta}+v_0+S\left[\left(\frac{r}{\gamma^2}v_{0\xi}-\frac{1}{r}u_{0\eta}\right)_\tau + V\left(\frac{r}{\gamma^2}v_{0\xi}-\frac{1}{r}u_{0\eta}\right)_\eta\right]=0. \quad (5.21)$$

The five equations (5.11), (5.12) and (5.19) to (5.21) in the five unknown variables u_0, v_0, p_0, w_1 and T_1 determine the stability problem. Since the coefficients depend solely on ζ, it is valid to assume a wave form for the perturbations

$$u_0=u_0(\zeta)\,e^{i(\sigma\tau+\eta+\xi)}, \quad \text{etc.,} \quad (5.22)$$

and we find

$$T_1=-\frac{i}{r}v_{0\zeta}, \quad (5.23)$$

$$v_0=-u_0=\frac{w_{1\zeta}}{1-S(r/\gamma^2+1/r)(\sigma+V)}, \quad (5.24)$$

which when substituted in the heat equation (5.20) yields

$$\left[(\sigma-\zeta+\tfrac{1}{2})\left(1-S\left(\frac{r}{\gamma^2}+\frac{1}{r}\right)(\sigma-\zeta+\tfrac{1}{2})\right)\right]w_{1\zeta\zeta} + \left[1-2S\left(\frac{r}{\gamma^2}+\frac{1}{r}\right)(\sigma-\zeta+\tfrac{1}{2})\right]w_{1\zeta} + r\theta\left[1-S\left(\frac{r}{\gamma^2}+\frac{1}{r}\right)(\sigma-\zeta+\tfrac{1}{2})\right]^2 w_1=0, \quad (5.25)$$

since

$$V=-(\zeta-\tfrac{1}{2}) \quad (5.26)$$

to this order of approximation.

VI. The stability equation

It is interesting to note that the basic state vertical velocity which was the motivation for choosing this model, does not appear in equation (5.25) and is not a source of instability. Furthermore, the latitudinal variation of the meridional velocity has been eliminated. We are left with a circulation consisting of isopycnal surfaces of constant slope and spacing, and a meridional velocity with vertical shear only.

Although the β-effect has been neglected as a stability feature in the mean state, it plays a significant role in the perturbation dynamics. It is important in the vorticity balance (the second term in (5.21)) and is of comparable magnitude to the local accelerations and mean state advection of the perturbation vorticity for this scale of motion.

The differential equation (5.25) is only of second order, but there are four boundary conditions to be satisfied, namely that w and T vanish at top and bottom. The equation was reduced in order from four to two by neglecting the diffusion terms containing the highest order derivatives in the heat equation (5.5). In general, boundary layers at $\zeta=0$ and $\zeta=1$ will be necessary to satisfy all the boundary conditions, with the "interior" solution being governed by (5.25).

It can be shown that the temperature boundary condition enters only in the calculation of higher order contributions to the eigenvalues, and that the correct boundary conditions that must be applied to the interior equation are

$$w=0 \text{ at } \zeta=0 \text{ and } \zeta=1. \quad (6.1)$$

Equation (5.25) contains the four non-dimensional numbers S, r, γ, and θ. However, if we introduce

$$p^2=\theta S\left(\frac{r^2}{\gamma^2}+1\right)=D^2(\lambda_0^2+\mu_0^2), \quad (6.2)$$

$$g=r\theta=D^2\frac{\beta}{V_0}\frac{\lambda_0}{\mu_0}, \quad (6.3)$$

where

$$D=\left(\frac{\alpha g(\Delta T)_v H}{f_0^2}\right)^{\frac{1}{2}} \text{ (the deformation radius of the basic stratified state)}, \quad (6.4)$$

the stability equation will contain only these two parameters, viz.

$$[(\sigma-\zeta+\tfrac{1}{2})(g-p^2(\sigma-\zeta+\tfrac{1}{2}))]\,w_{1\zeta\zeta} + [g-2p^2(\sigma-\zeta+\tfrac{1}{2})]\,w_{1\zeta} + [g-p^2(\sigma-\zeta+\tfrac{1}{2})]^2 w_1=0. \quad (6.5)$$

Equation (6.5) together with boundary conditions (6.1) will determine $\sigma=\sigma_r+i\sigma_i$ as a (multivalued) function of p and g. Of particular importance is the growth rate G which may be put into the useful form

$$G = \mu_0 V_0 \sigma_i(p_1 g) = \frac{V_0}{D}\left[\frac{1}{1+(Kg)^2}\right]^{\frac{1}{2}} p\sigma_i(p, g), \quad (6.6)$$

where
$$K = \frac{1}{D^2}\frac{V_0}{\beta}. \quad (6.7)$$

For the ocean, K is typically of the order of 0.1. The characteristic number B introduced in Part V is equal to $D^2\mu_0^2$, the square of the ratio between the deformation radius and the perturbation length scale.

From (6.5), it is easy to see that if σ is an eigenvalue, then so is its complex conjugate, σ^*, i.e., a decaying wave appears with an amplifying one. Under the transformation $g \to -g$, $\sigma \to -\sigma$, $\zeta' = 1 - \zeta$, equation (6.5) and (6.1) remain the same, and therefore $\sigma(g, p) = -\sigma(-g, p)$.

Thus the magnitude of σ_i depends only on p and the magnitude of g. Since all complex roots appear in conjugate pairs, $+g$ and $-g$ have the same growth rates (but opposite frequencies), and we may confine our stability analysis to positive g only.

The eigenvalue σ appears in (6.5) in a way such that even for fairly accurate estimates of the eigenfunction w_1, σ may have large errors. This is particularly true when σ_i is small and either $|\sigma_r| < \frac{1}{2}$ or $|\sigma_r - g/p^2| < \frac{1}{2}$ for in these cases, the coefficient of w'' will be small somewhere in the range of integration. The numerical method employed which achieved the required accuracy with relatively high economy was the Hamming (1959) predictor-corrector algorithm, a computationally stable procedure which seems very well suited to this type of boundary value problem. One further advantage is that spurious roots which solve less accurate finite difference equations do not enter. Over most of the parameter space it was found that a mesh spacing of $\Delta_\zeta = .02$ gave three place accuracy.

VII. The unstable field

The complex eigenvalue $\sigma(g, p)$ is shown in Figs. 2 and 3. Except for those wavelengths which lie on the p-axis above 2.40 and certain discrete lines, all waves are unstable. On these lines, which correspond to the integral values of the confluent hypergeometric parameter resulting from an analysis of the atmospheric baroclinic instability problem (Charney, 1947; Burger, 1962) the waves are neutral. In their vicinity, σ_r varies considerably.

We observe two different types of instability which are separated by the neutral line in Figs. 2 and 3:

(i) Those which join continuously to the line $p = 0$. These are precisely the geostrophic waves in the high wave number limit ($R_0 < \varepsilon < 1$) in equations (3.19) to (3.23) for the purely diffusive basic state (4.2), (4.3) (together with (2.15) and (2.16)). Note that although $\sigma_i \neq 0$, this is also a line of zero amplification (to this order in ε), since the growth rates are proportional to p (equation (6.6)).

(ii) Those which join continuously to the p-axis. The parameter g is the only term containing β, and the line $g = 0$ corresponds exactly (with the east–west and north–south wave numbers interchanged) to the baroclinic instabilities arising from a stratified circulation on an f-plane with a latitudinal density gradient, discussed by Eady (1949).

At this point it is appropriate to compare this formulation with the baroclinic instability problem solved by Green (1961). He chose a basic state consisting of an imposed north–south density gradient and the resultant zonal flow—the relevant problem for the atmosphere. It can be shown that Green's stability equation is equivalent to (6.5) for an incompressible fluid. There is a difference however in the parameters: g in equation (6.5) is in fact λ_0/μ_0 times the corresponding factor appearing in Green's model.

In the atmospheric problem then, the parameter g is a constant (depending only on basic state quantities) and it can be shown from the start that the wave number in the east–west direction must be zero at maximum growth rate. No such argument can be made in this problem where the parameters p and g both depend on the wave numbers. To find the maximum growth rate, we must locate the maximum value of (6.6) over all p and g (or λ_0 and μ_0) for given K (or equivalently for given D since we choose $V_0 = 1$ cm/sec).

We find that for a given g, the maximum instability is displayed by the type (ii) waves. The absolute maximum (over all p and g) occurs when $g = 0$ (and hence $\lambda_0 = 0$).

But this is precisely the result we would have obtained by ignoring the β-effect (for $\lambda_0 = 0$, the horizontal velocity is purely zonal). The fact

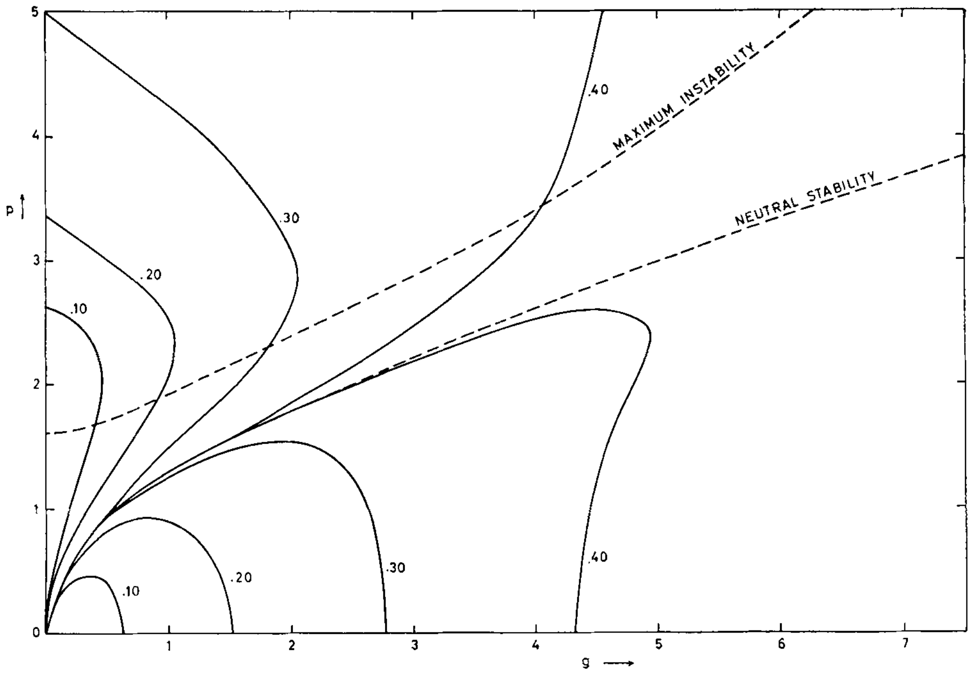

Fig. 2. Real part of σ. All waves are either unstable or neutral (the lower dashed line). On the upper dashed line, $p\sigma_1$ is a maximum for given g.

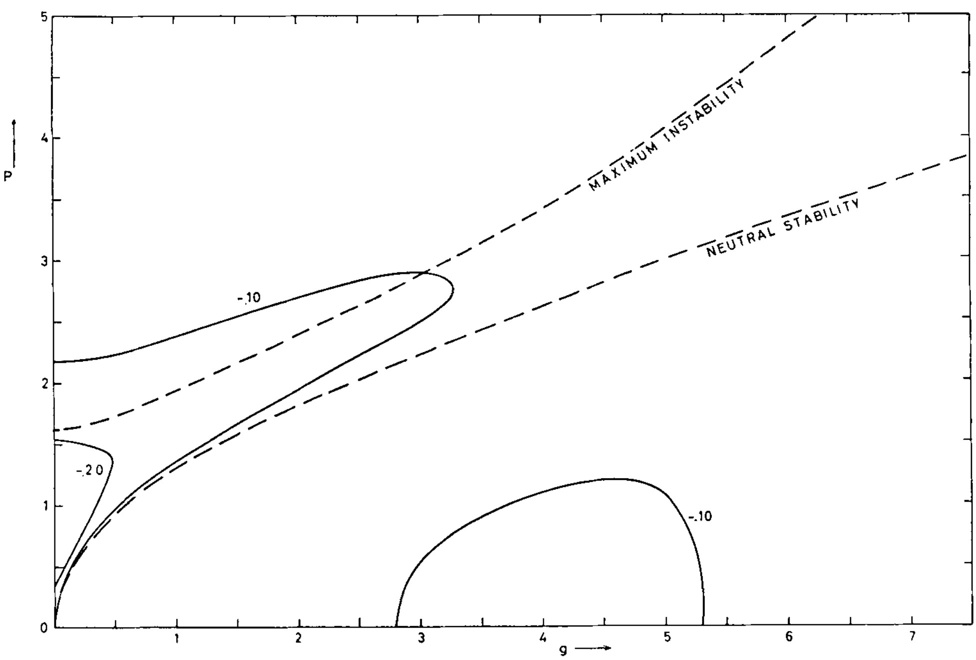

Fig. 3. Imaginary part of σ. See remarks to Fig. 2.

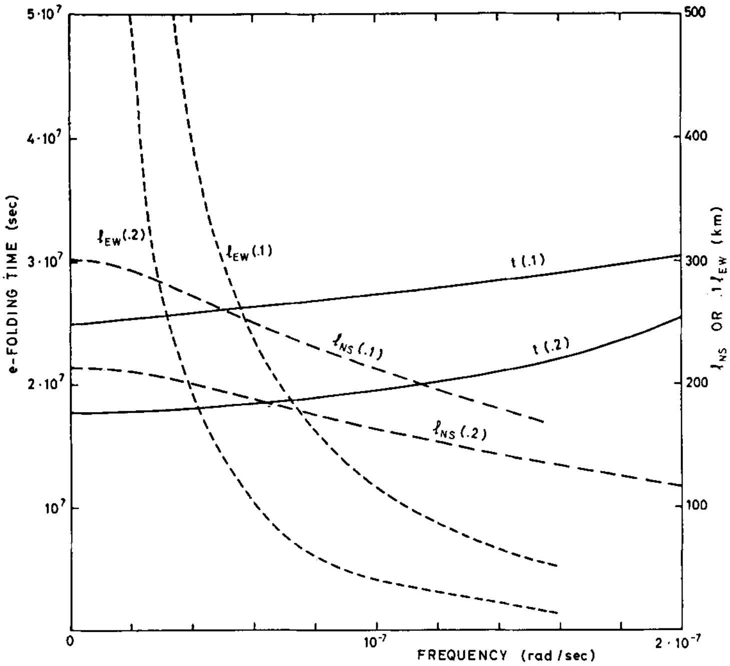

Fig. 4. Growth rates, frequencies, and wavelengths on maximum instability line, for the cases $K = 0.1$ and $K = 0.2$. The growth rates are expressed in terms of the e-folding time (full line). Note the difference in scale on the right-hand axis for the north–south wavelength (dashed line) and the east–west wavelength (dotted line).

that the perturbation motion is on the β-plane is irrelevant in so far as locating the absolute maximum growing wave, and β is a stabilizing effect.

However, this maximum is not a strong one, and there exists a curve $p = p(g)$, on which $p\sigma_i$ is a maximum for a given g (shown in Figs. 2 and 3) where the growth rate varies only slightly. For example, max $\{p\sigma_i\} = .287$ for $g = 5$ or only 7.6% less than for the maximum at $g = 0$. Off this line, the growth rates drop off more steeply. If amplification were plotted against p and g, this line would appear as a "ridge".

The typical density difference through the thermocline is 1.0×10^{-3} g/cm^3 in mid-latitudes and 2.0×10^{-3} in the sub-tropics. These correspond to $\theta = 5$, $D = 55$ km, $K \approx 0.2$ and $\theta = 10$, $D = 80$ km, $K \approx 0.1$ respectively for $f_0 = 10^{-4}$ sec^{-1}, $L = 6 \times 10^8$ cm, $H = 3 \times 10^5$ cm and $V_0 = 1$ cm/sec.

In Fig. 4, the dimensional growth rates (expressed as the e-folding time) and wavelengths are plotted versus the frequency for values lying on the "ridge" for the two cases $K = 0.1$ and $K = 0.2$. As can be expected, the less stably stratified ocean ($K = 0.2$) grows faster than the one for $K = 0.1$—about half a year and one year respectively.

At zero frequency, the growth rates and north–south wavelength achieve their maximum values. Also the east–west wavelength is infinite and the solution at this point of maximum instability corresponds to standing, non-oscillatory, amplifying waves, parallel to latitudinal lines.

The type (i) roots correspond to longer wavelength perturbations and are much less unstable. They are not included in Fig. 4 since their e-folding time is off the scale of the graph (i.e. greater than 5×10^7 sec).

It should be pointed out that the expansion carried out in Section V contained the implicit assumption that $r(=\gamma(\lambda_0/\mu_0))$ is an $0(1)$ quantity. It can be shown however that it is valid to consider waves with no longitudinal variation (those at maximum instability), simply by setting $r = 0$ in equation (5.25), or equivalently $g = 0$ in (6.5). They then reduce to

$$(\sigma + V)w'' + 2w' - S\theta(\sigma + V)w = 0, \quad (7.1)$$

the Eady (1947) stability equation.

VIII. Latitudinal variations

The above instabilities, obtained by assuming $f = 1$ and $\partial f/\partial \eta = \varepsilon$ are consistent only when $\eta^* = \varepsilon\eta < 1$. To extend the region of validity, introduce a new coordinate

$$\eta' = \int_0^\eta M(\eta^*)\, d\eta, \tag{8.1}$$

such that the perturbations are now of the form

$$\left.\begin{aligned} u &= u(\zeta, \eta^*)\, e^{i(\eta' + \xi + \sigma\tau)}, \\ v &= v(\zeta, \eta^*)\, e^{i(\eta' + \xi + \sigma\tau)}, \quad \text{etc.} \end{aligned}\right\} \tag{8.2}$$

The function $M(\eta^*)$ is to be determined so that the solution is uniformly valid when η^* is as large as 0(1). The variable η' is a slowly varying latitudinal distortion of the independent variable η and expresses the accumulative effect of integrating many waves over the full extent of the ocean. This approach is similar to that employed by Carrier (1966) in treating tsunami waves whose wavelength is small compared to the characteristic length scale of the bottom topography over which they are travelling.

Under the transformation (8.1), equations (5.1) to (5.5) may be expressed in terms of the new variable η'. All quantities, which are now considered as functions of both η^* and η' (the so-called *two-timing method*), are expanded in an ε-series.

$$u = u_0(\zeta, \eta^*; \eta') + \varepsilon u_1(\zeta, \eta^*; \eta') + \dots,$$

$$v = v_0(\zeta, \eta^*; \eta') + \varepsilon v_1(\zeta, \eta^*; \eta') + \dots, \quad \text{etc.} \tag{8.3}$$

and

$$M(\eta^*) = M_0(\eta^*) + \varepsilon M_1(\eta^*) + \dots.$$

Then to lowest order we have

$$v_0 = \frac{p_{0\xi}}{1 + \eta^*}, \tag{8.4}$$

$$u_0 = -\frac{M(\eta^*)}{1 + \eta^*}\, p_{0\eta'}, \tag{8.5}$$

and $w_0 = T_0 = 0$. Using the relationship

$$\frac{\partial}{\partial \eta} v = M \frac{\partial}{\partial \eta'} + \varepsilon \frac{\partial}{\partial \eta^*} v + \cdots$$

$$= M_0 v_{0\eta'} + \varepsilon \left(M_0 v_{1\eta'} + M_1 v_{0\eta'} + \frac{\partial}{\partial \eta^*} v_0 \right) + 0(\varepsilon^2), \tag{8.6}$$

going to first order in ε, and proceeding as in Section V, a single equation for w_1 may be obtained.

$$\begin{aligned} &(1+\eta^*)^2 \left[\left(\sigma + V_1(\zeta) \frac{M_0(\eta^*)}{1+\eta^*} \right) \left(1 - S \left(\frac{r}{\gamma^2} + \frac{M_0(\eta^*)^2}{r} \right) \right. \right. \\ &\times \left. \left. \left(\sigma + V_1(\zeta) \frac{M_0(\eta^*)}{1+\eta^*} \right) \right) \right] w_{1\zeta\zeta} + (1+\eta^*) M_0(\eta^*) \\ &\times \left[1 + S \left(\frac{r}{\gamma^2} + \frac{M_0(\eta^*)^2}{r} \right) \left(\sigma + V_1(\zeta) \frac{M_0(\eta^*)}{1+\eta^*} \right) \right. \\ &\times \left. (V_1'(\zeta) - 1) \right] w_{1\zeta} + r\theta \left[1 - S \left(\frac{r}{\gamma^2} + \frac{M_0(\eta^*)^2}{r} \right) \right. \\ &\times \left. \left(\sigma + V_1(\zeta) \frac{M_0(\eta^*)}{1+\eta^*} \right) \right]^2 w_1 = 0 \end{aligned} \tag{8.7}$$

where $V_1(\zeta) = -(\zeta - \frac{1}{2})$.

This equation must be solved with the boundary conditions $w_1(0) = w_1(1) = 0$, under the constraint that σ be a constant over the physical space. However, no general solutions $M(\eta^*)$ were found which allow σ to be independent of η^*, indicating that the correct latitudinal dependence is perhaps more complicated than the assumed wave form (8.2).

Fortuitously, one special case can be solved, namely, when $r = 0$, that is, no longitudinal variation of the perturbation variables. This is in fact the condition at which maximum instability occurs under the "local" hypothesis. In the limit $r \to 0$ (8.7) becomes

$$\begin{aligned} &(1+\eta^*)^2 \left(\sigma + V_1(\zeta) \frac{M_0(\eta^*)}{1+\eta^*} \right) w_{1\zeta\zeta} \\ &+ 2(1+\eta^*) M_0(\eta^*) w_{1\zeta} - M_0(\eta^*)^2 \theta S \\ &\times \left(\sigma + V_1(\zeta) \frac{M_0(\eta^*)}{1+\eta^*} \right) w_1 = 0. \end{aligned} \tag{8.8}$$

For the choice

$$M_0(\eta^*) = 1 + \eta^*, \tag{8.9}$$

i.e.

$$\eta' = \eta \left(1 + \frac{\eta^*}{2} \right), \tag{8.10}$$

the coefficients containing η^* in (8.22) cancel, and it reduces to Eady's (ordinary) differential equation,

$$(\sigma - \zeta + \tfrac{1}{2})\, w_{1\zeta\zeta} + 2w_1 - \theta S(\sigma - \zeta + \tfrac{1}{2})\, w_1 = 0. \tag{8.11}$$

Hence, in the special case $r = 0$, the growth rates remain as before, but now the north–south wavelength varies with latitude. From (8.24),

$$l_{NS} = \frac{2\pi}{\mu_0} \frac{1}{(1+\eta^*/2)}, \tag{8.12}$$

i.e., the wavelength is $\frac{1}{3}$ shorter at $\eta^* = 1$ and twice as long at $\eta^* = -1$, than at $\eta^* = 0$, the mid-latitude of the ocean.

IX. Conclusions

The amplifications associated with the baroclinic unstable waves are small (0(1 year)) and do not possess a sharp maximum with respect to the parameters. We can expect, therefore, that a whole class of waves, and not simply one combination, will manifest itself in the ocean circulation. Those perturbations whose amplification is near the maximum growth rate (i.e., on the ridge line) have a smaller north–south wavelength than does the perturbation actually at the maximum. We expect, then, that the latter wavelength serves as an effective upper bound on the north–south wavelengths, and we would expect most perturbations to be of this order—several hundred kilometers for the values of the parameter K chosen. However, there is little selectivity in the east–west wavelength. It can vary by several orders of magnitude without significantly affecting the growth rates, and no meaningful predictions can be made on the basis of the analysis. Similarly, the amplification near the maximum growth rate is not strongly dependent on the frequency for values of the latter in the range 0 to 10^{-7} sec^{-1} (corresponding to periods of greater than two years).

The above growth rates and frequencies are so small, we could not expect to find instabilities which have actually grown from an infinitesimal disturbance to the observed magnitudes. The ocean is not a well-controlled laboratory flow, and is incapable of maintaining a steady circulation, such as our posited basic state, over many years. However, since the perturbations are very nearly neutral, if a finite amplitude disturbance of the correct scale were introduced into the ocean, we would expect that disturbance to keep its character for a considerable time before it decayed. Fluctuations in the Gulf Stream might be an example of such a phenomenon, and the possibility exists that its meanders are an important energy source of the mid-ocean transient circulation.

Table 1

H	V_0	ns	e-folding time
1 km	31.6 km	124 km	1.02×10^7 sec
2	44.7	176	1.44
3	54.8	215	1.77
4	63.2	248	2.04
5	70.7	278	2.28

We have approximated the thermocline by a linear density gradient from top to bottom, whereas in fact, it is more boundary layer-like in character, with a characteristic scale of about one kilometer. We have chosen a value of H intermediate to the thermocline depth and the total depth of the ocean, and it is instructive to compare the results for different H. Table 1 is constructed at the maximum unstable point ($g = 0$, $p = 1.6$) for the value $V_0 = 1$ cm/sec.

The table was constructed at a constant value of V_0 to reveal the dependence on H alone. But note that the growth rate is linearly proportional to V_0. The results presented here are valid for basic states which are predominantly diffusive, i.e., $\wedge \lesssim 5$. Thus for $\varkappa = 50\,\text{cm}^2/\text{sec}$ and $H = 1$ km, it is possible for V_0 to be as large as 7.5 cm/sec. This corresponds to an e-folding time of only $.14 \times 10^7$ sec or $2\frac{1}{2}$ weeks. Since frequency has the same H dependence as the growth rate, a period of two years for $H = 3$ km corresponds to a possible minimum period of seven weeks at $H = 1$ km. Care must be taken not to attach too much importance to these values, since the boundary condition, $w = 0$ at a depth of one kilometer is unrealistic. These calculations have been introduced to exhibit the limitation of a linear thermocline extending to the bottom of the ocean. *It is speculated that an analysis of a more realistic thermocline will yield higher growth rates.*

We note that for all wavelengths and modes σ_r is always positive. Through symmetry arguments of Chapter III, Section 4, it can be shown that these amplifying waves can thus have only a westward component of phase velocity and correspond to Rossby waves for large wavelengths. Similarly, both north and southward components are possible, and in fact equally likely, since they have the same growth rate.

The presence of a constant east–west wind at the surface of the ocean does not alter the stability of the circulation. It forces a vertical velocity at the bottom of the Ekman layer: $w = \nabla\times(\tau/f) = \beta/f^2(\tau_0)$. In the high wave number limit, the parameter $\chi = \tau_0/f_0 H v_0$, appears only in combination with the eigenvalue σ such that the problem is unchanged if we replace $\sigma + \chi$ by σ', i.e., wind changes only the frequency, not the growth rates. In this case, the absolute instability maximum ($g = 0$, $p = 1.6$) actually has an oscillatory character with time dependence $\exp\{i(p/D)(\tau_0/f_0 H)t\}$. However, for $\tau_0 = 1$ cm^2/sec^2, a typical oceanic value, the associated period is very large (0(20 years)), from which we conclude that if wind were to be an important effect in the model, a time-dependent, or possibly a spatially varying one, must be considered.

On the ridge line, the growth rate is a maximum at $g = 0$ and decreases slowly as g increases. The β term appears only in g and is thus a slight stabilizing effect.

Crease (1962) observed that the deep currents are primarily longitudinal. This feature is not explained by the present theory; on the contrary, we find that as $g \to 0$ (or $r \to 0$), the ratio of the meridional to zonal dimensional velocity component is $0(\varepsilon)$. This difference is perhaps traceable to our choice of a basic state with a strong east–west density gradient throughout the ocean.

In this problem, with an east–west density gradient as well as the Green-Eady one with a north-south gradient, the maximum instability is characterized by waves with no variation in the direction of the gradient. If we consider the situation in which the density gradient is at an angle α with respect to a longitudinal line, it can be shown that we are led to the same differential equation (and boundary conditions) as (6.5), but the parameters are now

$$p^2 = D^2(\lambda_0^2 + \mu_0^2), \tag{9.1}$$

$$g = D^2 \frac{\beta}{V_0}\left(\frac{\lambda_0}{-\lambda_0 \cos\alpha + \mu_0 \sin\alpha}\right) \tag{9.2}$$

and the growth rate

$$G = |\lambda_0 \cos\alpha - \mu_0 \sin\alpha| v_0 \sigma_i(p_1 g), \tag{9.3}$$

where λ_0 and μ_0 are the dimensional east–west and north–south wave numbers, and σ_i is the computed function graphed in Fig. 3.

Note that $\alpha = 0$ is Green's model of the atmosphere, and $\alpha = \pi/2$ is the configuration discussed in this paper. When $\alpha \neq 0$ it is unclear how to decide *ab initio* where the maximum growth lies in wave number space. It is speculated that it will lie with zero wave number in the direction of the density gradient (as is the case in this and Eady's problem), i.e.,

$$\lambda_0 \sin\alpha + \mu_0 \cos\alpha = 0, \tag{9.4}$$

but this computation has yet to be performed.

Detailed comparison between these results and the real ocean must await a systematic exploration (spatial and temporal) of the actual intermediate scale phenomena. The frequencies observed in the ocean are somewhat higher than those predicted in this paper. However, the north-south wavelength calculated here agrees with the limited measurements taken to date.

REFERENCES

Burger, A. P. 1962. On the non-existence of critical wavelengths in a continuous baroclinic stability problem. *Journal of the Atmospheric Sciences 19*, 30.

Carrier, G. F. 1966. Gravity waves on water of variable depth. To appear in *Journal of Fluid Mechanics*.

Charney, J. G. 1947. The dynamics of long waves in a baroclinic westerly current. *Journal of Meteorology 4*, 135.

Crease, J. 1962. Velocity measurements in the deep water of the western North Atlantic. *Journal of Geophysical Research 67*, 3173.

Day, C. G. & Webster, F. 1965. Some current observations in the Sargasso Sea. *Deep Sea Research 12*, 805.

Defant, A. 1961. *Physical Oceanography*, Vol. 1. Pergamon Press, New York.

Eady, E. T. 1949. Long waves and cyclone waves. *Tellus 1*, 33.

Green, J. S. A. 1960. A problem in baroclinic stability. *Quarterly Journal of the Royal Meteorological Society 86*, 237.

Hamming, R. W. 1959. Stable predictor-corrector methods for ordinary differential equations. *Journal of the Association for Computing Machinery 6*, 37.

Phillips, N. A. 1963. Geostrophic motion. *Reviews of Geophysics 1*, 123.

Reid, J. L. 1965. *Intermediate Waters of the Pacific Ocean*. The Johns Hopkins Press, Baltimore.

Robinson, A. R. 1962. The instability of a thermal ocean circulation. *Journal of Marine Research 20*, 189.

Robinson, A. R. & Stommel, H. 1959. The ocean thermocline and the associated thermohaline circulation. *Tellus 11*, 295.

Swallow, J. C. 1955. A neutral-boyancy float for measuring deep currents. *Deep Sea Research 3*, 74.

Welander, P. 1959. An advective model of the ocean thermocline. *Tellus 11*, 309.

БАРОКЛИННАЯ НЕУСТОИЧИВОСТЬ ОКЕАНИЧЕСКОЙ ЦИРКУЛЯЦИИ

Неустойчивость потока, моделирующего линейный океанический термоклин, исследуется с точки зрения понимания возмущений промежуточного масштаба, наблюдавшихся Крисом (1962) и другими. Анализ Робинсона (1962) устойчивости термической океанической циркуляции обобщен с целью включения усиливающихся квазигеострофических возмущений. Предсказаны длины волн с севера на юг, порядка нескольких сотен километров, согласующиеся с предыдущими измерениями.

Для специального случая возмущений, не зависящих от долготы, получено решение для океанов с большими размерами по широте. Скорости возрастания амплитуды имеют порядок года, длина волны с севера на юг является функцией широты.

Хотя выбранное основное состояние отличается от соответствующего атмосферного аналога, исследованного Иди (1949) и Грином (1960), оба состояния являются бароклинно-неустойчивыми и имеют возмущения с аналогичными свойствами. При максимальной неустойчивости оба они содержат возмущения, постоянные в направлении, параллельном широтному градиенту плотности основного потока, и этот результат верен как на f-плоскости, так и на β-плоскости.

20 – 662898